Analytical and computational study of self-induced transparency mode locking in quantum cascade lasers

Muhammad Anisuzzaman Talukder[*] and Curtis R. Menyuk[†]

Department of Computer Science and Electrical Engineering, University of Maryland, Baltimore County, 1000 Hilltop Circle, Baltimore, Maryland 21250, USA

The possibility of using the self-induced transparency effect to achieve laser mode locking has been discussed since the late 1960s but has never been observed. In prior work, we proposed that quantum cascade lasers are the ideal tool to realize self-induced transparency mode locking due to their rapid gain recovery times and relatively long coherence times, and because it is possible to interleave gain and absorbing periods. Here, we present designs of quantum cascade lasers that satisfy the requirements for self-induced transparency mode locking at both 8 and 12 μm, indicating that it is possible to satisfy these requirements over a wide wavelength range. The coupled Maxwell-Bloch equations that define the dynamics in quantum cascade lasers that have both gain and absorbing periods have been solved both analytically and computationally. Analytical mode-locked solutions have previously been found under the conditions that there is no frequency detuning, the absorbing periods have a dipole moment twice that of the gain periods, the input pulse is a π pulse in the gain medium, and the gain recovery times in the gain and absorbing periods are much longer than the coherence time T_2 and are short compared to the round-trip time. It was shown that the mode-locked pulse durations are on the order of T_2, which is typically about 100 fs in quantum cascade lasers. In this work, these analytical results are reviewed and extended to include the effects of partial inversion in the gain and absorbing periods and of frequency detuning. An energy theorem in the limit of long coherence times is derived. The Maxwell-Bloch equations have been solved computationally to determine the robustness of the mode-locked solutions when frequency detuning is present, the dipole moment of the absorbing periods differs from twice that of the gain periods, the gain relaxation time is on the order of 1–10 ps, as is typically obtained in quantum cascade lasers, and the initial pulse is not a π pulse in the gain medium. We find that mode-locked solutions exist over a broad parameter range. We have also investigated the evolution of initial pulses that are initially much broader than the final mode-locked pulses. As long as the initial pulse duration is on the order of T_1 or shorter and has enough energy to create a π pulse in the medium, a mode-locked pulse with a duration on the order of T_2 will ultimately form.

I. INTRODUCTION

McCall and Hahn [1,2] observed that a pulse with a duration τ that is short compared to the coherence time T_2 of a saturable resonant medium will pass through the medium as if the medium were transparent, as long as the pulse energy exceeds a critical value. They gave this effect the name self-induced transparency (SIT). When the pulse energy is below the critical value, the pulse damps. SIT reshapes pulses in the correct energy range, so that they have a hyperbolic-secant shape with a well-defined energy and duration. This effect has been used for pulse compression [3,4], and these pulses are referred to as 2π pulses.

Self or passive mode locking of lasers [5,6] was discovered experimentally at almost the same time as SIT, and there was speculation that the mode locking was due to SIT [7,8]. However, subsequent work made it clear that SIT could not account for the observed mode locking [9,10]. Conventional passively mode-locked systems operate in regimes in which the pulse bandwidth is smaller than the gain bandwidth, so that typically coherence times T_2 are short

compared to the pulse duration. With the development of the standard theory of passive mode locking [11], work on SIT mode locking almost ceased. An exception is work by Kozlov [12], who pointed out the importance of including an absorbing medium, in which the pulse is a 2π pulse, along with a gain medium in which the pulse is a π pulse. The absorbing medium acts as a saturable absorber suppressing the generation of continuous waves and the Risken-Nummedal-Graham-Haken (RNGH) instability [13].

Quantum cascade lasers (QCLs) [14] are important light sources in the midinfrared range. The light is generated by a transition between two subbands in the conduction band, in contrast to interband semiconductor lasers. As a consequence, the subbands have narrow linewidths and long coherence times T_2 compared to interband semiconductor lasers. Values of T_2 on the order of 100 fs are achievable [15]. Another important feature of the QCLs is their rapid gain recovery times T_1 compared to interband semiconductor lasers due to fast LO-phonon relaxation. Typical values of T_1 are in the range 1–10 ps, which is short compared to T_{rt}, the round-trip time in the cavity [15]. Typical values of T_{rt} are on the order of 50 ps.

The narrow linewidths and fast recovery times of QCLs make it difficult to achieve conventional passive mode locking. Gain bandwidths that are significantly larger than the

---

[*]anisuzzaman@umbc.edu

[†]menyuk@umbc.edu

pulse bandwidths are required, and that is hard to obtain when the linewidths are narrow, as in QCLs. A saturable gain, with a recovery time that is long compared to T_{rt}, is also required for conventional mode locking in order to suppress continuous waves, and the typical gain recovery times in QCLs are shorter than the round-trip times. Thus, conventional passive mode locking cannot work in QCLs that operate in a standard parameter regime.

In prior work [16], we proposed that QCLs are an ideal tool for creating the long-predicted, never-observed SIT mode locking. The relationship $T_2 \ll T_1 \ll T_{rt}$, which is typical for QCLs, is precisely what is needed for SIT mode locking, and the ease of band-gap engineering in QCLs makes it possible to interleave gain and absorbing periods as needed. Conversely, SIT mode locking of QCLs makes it possible in principle to obtain mode-locked pulses from a midinfrared laser that are less than 100 fs in duration. In this work, we extend our prior work to show that these results are robust over a broad parameter range.

In related work, Wang *et al.* [17] and Gordon *et al.* [18] observed the Risken-Nummedal-Graham-Haken instability in QCLs with only gain periods and they modeled their QCLs using the two-level approximation of the Maxwell-Bloch equations. They did not find it necessary to include chromatic dispersion. They did, however, include a saturable nonlinearity. By carefully separating this effect from the effect of spatial hole burning, Gordon *et al.* [18] showed that its quantitative impact can be significant, but it does not affect the qualitative results. They attributed the saturable nonlinearity to effects that depend on the detailed geometry of the QCL. By contrast, spatial hole burning qualitatively changes the evolution of the RNGH instability and can completely suppress it. However, in SIT mode locking, continuous waves are suppressed and the mode-locked pulses propagate in one direction or the other at any one time so that spatial hole burning is not an issue. We conclude that the two-level Maxwell-Bloch equations are an adequate model for QCLs in the parameter regime of interest for SIT mode locking.

More recently, Wang *et al.* [19] obtained 3 ps pulses in an actively mode-locked system and Choi *et al.* [20] demonstrated SIT-related coherence by injecting 200 fs pulses into a QCL. Like many passively mode-locked lasers, an SIT-mode-locked QCL will not self-start. These works suggest that it may be possible to start the SIT mode locking either by injection locking or by actively modulating it. It might also be possible to use mechanical or electrical perturbations to start the mode locking.

The stability of SIT mode locking depends on the magnitude of the gain per unit length relative to the absorption per unit length and the linear loss per unit length. In this study, we treat these quantities as parameters; we do not calculate them from first principles. While the gain and absorption per unit length will be roughly proportional to the current, their relative magnitude is not easy to calculate. This magnitude depends on the carrier distribution and coherence times in all the levels in both the QCL's active and injector regions, and must be calculated using a Monte Carlo, quantum kinetic density matrix, or a nonequilibrium Green's function approach [21–24].

The remainder of this paper is organized as follows: in Sec. II, we give a physical picture of how SIT mode locking works. In Sec. III, we present realistic QCL structures designed to operate at 8 and 12 μm that satisfy the design requirements that the dipole moment in the absorbing periods is approximately twice that of the gain periods and the resonant frequencies are nearly equal. These results indicate that it is possible to satisfy the requirements for SIT mode locking over a broad parameter range [25]. In Sec. IV, we present the Maxwell-Bloch equations and discuss analytical solutions of these equations. Prior work [16] is reviewed and extended and an energy theorem is derived. In Sec. V, we present a detailed computational study of the Maxwell-Bloch equations that shows that SIT mode locking is robust when the parameter values change from the ideal values for which analytical solutions can be found. Finally, Sec. VI contains a discussion of our results.

II. PHYSICAL PICTURE OF SIT MODE LOCKING

In order to obtain SIT mode locking, it is necessary to have two highly coherent resonant media with nearly equal resonant frequencies. In one medium, denoted the gain medium, electrons should be injected into the upper lasing state so that the resonant states are nearly inverted. In the other medium, denoted the absorbing medium, electrons should be injected into the lower state so that the resonant states are not inverted. Also, the dipole strength in the absorbing medium should be nearly equal to twice the dipole strength in the gain medium. At the same time, the ratio of the gain per unit length to the absorption per unit length should be small enough so that the growth of continuous waves is suppressed, but large enough so that a mode-locked pulse can stably exist. It is possible to simultaneously satisfy all these conditions by interleaving gain and absorbing periods that have the required dipole strengths as shown schematically in Fig. 1. By appropriately choosing the number of gain periods and the number of absorbing periods, one can in principle obtain any desired ratio for the gain and absorption per unit length. As long as there are many periods within the transverse wavelength of the lasing mode, the gain and absorbing periods will experience the same light intensity.

In Fig. 2, we show simplified two-level resonant structures for the gain and absorbing media. In the gain medium, electrons are injected into level 2g and are extracted from level 1g. The carrier lifetime in 2g should be longer than the mode-locked pulse duration and the equilibrium population inversion should be nearly complete. When an optical pulse with a photon energy equal to the resonant energy impinges on the gain medium with its polarization oriented in the direction perpendicular to the layers, electrons scatter to level 1g and photons are emitted. Then, the electrons are nonradiatively extracted from level 1g. In the absorbing medium, electrons are injected into the lower level 1a. The lifetime of state 1a should again be longer than the pulse width. When a light pulse of the appropriate wavelength and polarization impinges on the absorbing medium, photons are absorbed and electrons jump to level 2a. If a light pulse has enough intensity, then photons are re-emitted with no overall loss in
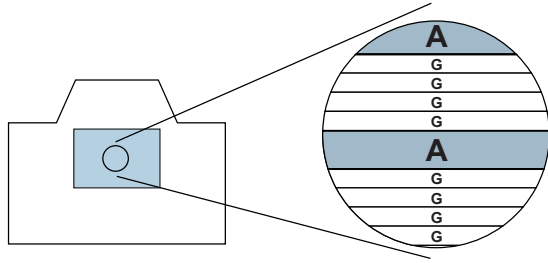
FIG. 1. (Color online) Schematic of a QCL structure with gain and absorbing periods. On the left, we show a cutaway view of the QCL structure. The active region is shown as a filled-in rectangle. We are looking in the direction along which light would propagate. Electrodes would be affixed to the top and bottom so that electrons flow vertically. The heterostructure would also be stacked vertically as shown on the right. We show one absorbing period for every four gain periods, corresponding schematically to the case in which the electron density in the gain medium (N_g) $\simeq 4 \times$ the electron density in the absorbing medium (N_a), and we show absorbing periods that are twice as large as gain periods to indicate schematically that the dipole moment in the absorbing medium (μ_a) $\simeq 2 \times$ the dipole moment in the gain medium (μ_g).

one Rabi oscillation time. In order for these processes in the gain medium and absorbing medium to occur simultaneously, the energy spacing between the resonant levels should be nearly the same in both media.

In the theory of resonant two-level media, both π pulses and 2π pulses play an important role [26]. A π pulse is a pulse with sufficient energy to exactly invert the lower state population of a two-level medium if the medium is initially uninverted, or, conversely, to uninvert the upper state if the medium is initially inverted. In the former case, the pulse experiences loss and rapidly attenuates, but, in the latter case, the pulse experiences gain. The pulse duration is approximately half a Rabi oscillation period. If a pulse lasts a longer time than required to drive the population from the upper level to the lower, then the medium will amplify the first part of the pulse and attenuate the latter part, in a way that shortens the pulse. Conversely, if a pulse is initially too short, it is lengthened. Because a π pulse experiences gain, it is natural that shortly after the initial observations of passive mode locking in lasers, it was proposed that the pulses in these lasers are actually SIT-induced π pulses [7,8]. However, these pulses are not suitable for use on their own as passively mode-locked laser pulses. Where one π pulse can exist, there is nothing to prevent continuous waves from generating multiple pulses leading to chaos rather than a single stable pulse oscillating in a laser cavity.
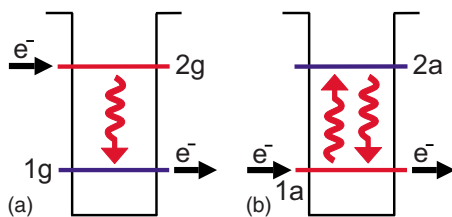

FIG. 2. (Color online) Schematic of the (a) gain and (b) absorbing media. Black straight-line arrows indicate the direction of electron flow. Red wavy arrows indicate radiative transitions.

One can in principle circumvent this difficulty by combining a gain medium in which the optical pulse is a π pulse with an absorbing medium in which the optical pulse is a 2π pulse [10]. A 2π pulse is a pulse with sufficient energy so that in an uninverted medium the lower state population is first inverted and then returned to the lower state in approximately one Rabi oscillation. A 2π pulse like a π pulse is stable. If its initial duration is too long, the duration decreases, and, if its initial duration is too short, the duration increases. The 2π pulse propagates through the medium without loss, in contrast to continuous waves at the resonant optical frequency, which experience loss. This remarkable property is what led to the name "self-induced transparency" [1,2]. Because of this property, the absorbing medium acts like the saturable loss in a conventional passively mode-locked system, suppressing the growth of continuous waves, while allowing a short pulse to propagate.

It is evidently important that both the gain medium and the absorbing medium act on the optical pulse simultaneously. We may achieve this simultaneous interaction by designing a QCL structure that has the gain and absorbing periods interleaved along the growth axis of the structure, as shown in Fig. 1. By making the dipole moment in the absorbing periods twice that of the gain periods, a π pulse in the gain periods is a 2π pulse in the absorbing periods. Therefore, an injected π pulse completely depletes the gain medium as it makes its way through the QCL, whereas, the absorbing medium becomes transparent. We will show that by controlling the amount of gain and absorption per unit length in the gain and absorbing media, pulse durations can be controlled.

In order to suppress spatial hole burning, the RNGH instability, or the growth of multiple pulses, we do not want continuous waves to grow in an SIT mode-locked laser. The absorption parameter should be large enough to keep the laser operating below the threshold for the growth of continuous waves. Therefore, the laser cannot self-start and it is necessary to use external means to start the mode locking. Essentially, we need a seed pulse that has sufficient energy and a duration on the order of T_1. We suggest two optical approaches. First, we can seed the pulse from an external source by injection locking, or, second, we can use active mode locking to generate an initial pulse that will have a suitable energy and initial duration for SIT mode locking. It may also be possible to use a mechanical or an electrical impulse to start the mode locking.

III. QUANTUM CASCADE LASER STRUCTURES

We have designed QCL gain and absorbing periods that fulfill the SIT mode locking requirements at two different wavelengths, 8 and 12 μm. Similar structures can be designed over a broad range of mid-ir wavelengths [25]. We use the $In_{0.52}Al_{0.48}As/In_{0.53}Ga_{0.47}As$ material system for the active region in our design since most of the demonstrated QCLs to date have been based on this material system. However, mode-locking structures operating at less than 8 μm will be difficult to design using this material system. Since electrons are injected into the lower state in the absorbing
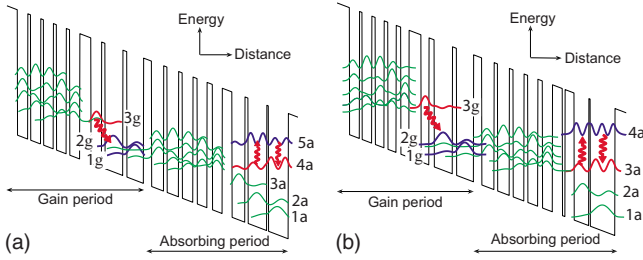
FIG. 3. (Color online) Conduction-band diagram and moduli-squared wave functions for one gain and one absorbing period of the (a) 12 μm, (b) 8 μm mode-locking QCL structures. The sequence of layer dimensions is (in Å, starting from left): (a) **37**, 36, **10**, 35, **10**, 34, **11**, 34, **12**, 35, **39**, 37, **12**, 62, **14**, 58, **28**, 42, **12**, 40, **13**, 37, **15**, 34, **15**, 34, **34**, 45, **11**, 65, **6**, 69; (b) **42**, 34, **9**, 33, **12**, 30, **13**, 28, **16**, 28, **41**, 27, **18**, 62, **14**, 58, **28**, 42, **12**, 40, **13**, 37, **13**, 34, **16**, 34, **34**, 9, **31**, 50, **5**, 84. The numbers in bold type indicate In$_{0.52}$Al$_{0.48}$As barrier layers and those in roman type indicate In$_{0.53}$Ga$_{0.47}$As well layers. Red wavy arrows indicate radiative transitions.

medium, the upper state approaches close enough to the conduction-band edge at wavelengths below 8 μm to lead to a large increase in the carrier loss due to scattering to the continuumlike states. To design a mode-locking structure at shorter wavelengths, it should be possible to use a strain-balanced InAlAs/InGaAs material system.

The gain periods in our design are typical QCL periods. We design a three-quantum-well active region for the gain periods that has a diagonal transition, which lowers the dipole moment relative to designs that have a vertical transition. This choice simplifies the design of the absorbing periods. Population inversion is achieved by confining the resonant states in separate quantum wells and depopulating the lower state through phonon relaxation to another state sitting below the lower resonant state. While the dipole moment in the gain periods is not high, the upper state lifetime is larger than in the case of vertical transitions so that the gain remains high. The design of absorbing periods is different from the design of gain periods. The combined requirements of carrier injection into and extraction from the lower resonant level and a dipole moment twice that of the gain periods make it difficult to design the absorbing periods. To achieve a large dipole moment, the transition should be between two excited states. The carrier lifetime is made high by reducing scattering through phonon relaxation and reducing the carrier tunneling from the lower resonant state into the succeeding injector states. The injector regions have different designs when the electrons are tunneling into a gain or absorbing active region due to the different quantum electronic structures of gain and absorbing active regions.

The structure in Fig. 3(a) emits light at 12 μm. Electrons are injected into level 3g, and the gain transition is between levels 3g and 2g. The dipole moment between the resonant levels is given by $\mu_g/e = 1.81$ nm. Level 3g has a lifetime of $\sim$2 ps. Level 1g is positioned approximately at phonon resonance with 2g. Level 2g has a lifetime of $\sim$0.5 ps, so that the population inversion is high. The transition energy is 101 meV. In the absorbing periods, electrons are injected into level 4a and they jump to level 5a by absorbing photons. The

lifetime of level 5a is $\sim$0.83 ps. The absorbing levels are separated by 101 meV and have a dipole moment $\mu_a/e = 3.65$ nm. After electrons are injected into level 3g, they have a long lifetime of 2 ps due to the low scattering rate. When the optical pulse arrives, the population in level 3g decreases to level 2g. Level 2g is depopulated quickly to level 1g through phonon interactions and the electrons then transit to the following injector stage. Population inversion is restored before the optical pulse makes a round trip in the laser cavity. Electrons sit in level 4a after being injected by the preceding injector stage. When an optical pulse reaches the absorbing periods, electrons from level 4a move to level 5a by absorbing photons. Since the pulse is a 2π pulse for the absorbing medium, level 5a is depleted by making a Rabi oscillation, during which photons are emitted.

In the structure given in Fig. 3(b), the gain transition is between levels 3g and 2g. The dipole moment between the gain levels is 1.55 nm and the lifetime of level 3g is $\sim$3 ps. The resonant transition energy is 150 meV in both the gain and absorbing periods. In this structure, electrons are injected into level 3a in the absorbing periods and the absorbing transition is between levels 3a and 4a. Level 4a has a lifetime of $\sim$0.8 ps. The absorbing levels have a dipole moment $\mu_a/e = 2.95$ nm.

In a QCL, the time T_1 is determined mainly by the LO-phonon relaxation rate. The LO-phonon relaxation rate depends mainly on the energy spacing between the levels and the overlap of the corresponding wave functions, so that T_1 depends on the details of the band structure and can vary greatly from design to design. Indeed, strictly speaking there is not a single T_1 in either the gain or the absorbing medium since there are more than two levels involved in the dynamics in both media. In the gain stage of the QCL structure given in Fig. 3, the upper state is confined in a separate quantum well from the other states in the active region, so that the phonon relaxation rate is smaller than when all the active states are in the same well and the lifetime is higher. However, the absorbing stage is designed such that the upper and lower state wave functions have a large overlap, which makes the dipole moment higher, but decreases the lifetime. Therefore, in practical designs, we find $T_{1g} > T_{1a}$.

Generally, if the gain and absorbing media are grown from the same material system, it is reasonable to assume $T_{2g} \approx T_{2a}$. In the QCL structure that we propose, an In$_{0.52}$Al$_{0.48}$As/In$_{0.53}$Ga$_{0.47}$As material system is used for both the gain and absorbing periods, so that T_{2a} should not vary much from T_{2g}. However, there has yet to be a detailed theoretical calculation of these coherence times. In a QCL, the value of T_2 depends mainly on electron-electron scattering, electron–LO-phonon scattering, and interface scattering. Therefore, the values of T_{2g} and T_{2a} may differ somewhat, depending on the details of the design.

IV. MAXWELL-BLOCH EQUATIONS

Wang *et al.* [17] and Gordon *et al.* [18] have observed the RNGH instability in QCLs with only gain periods. They showed evidence for Rabi oscillations and demonstrated that the two-level Maxwell-Bloch equations apply to QCLs in

some parameter regimes, although they also showed that saturable absorption affects the behavior quantitatively, significantly reducing the RNGH threshold. Gordon et al. [18] attributed the saturable absorption to Kerr lensing that increases the mode overlap with the active region and reduces the wall losses. These effects depend sensitively on the details of the QCL geometry. They also observed that spatial hole burning due to the interaction of forward- and backward-propagating waves has an important effect on the pulse spectrum. They did not find it necessary to include chromatic dispersion or other nonlinearities. Motivated by these results, we use a simple two-level model based on the standard one-dimensional Maxwell-Bloch equations [26,27]. The Maxwell-Bloch equations that describe the light propagation and light-matter interaction in QCL having interleaved gain and absorbing periods may be written as

$$\frac{n}{c}\frac{\partial E}{\partial t} = -\frac{\partial E}{\partial z} - i\frac{kN_g\Gamma_g\mu_g}{2\epsilon_0 n^2}\eta_g - i\frac{kN_a\Gamma_a\mu_a}{2\epsilon_0 n^2}\eta_a - \frac{1}{2}lE, \quad (1a)$$

$$\frac{\partial \eta_g}{\partial t} = \frac{i\mu_g}{2\hbar}\Delta_g E - \frac{\eta_g}{T_{2g}}, \quad (1b)$$

$$\frac{\partial \Delta_g}{\partial t} = \frac{i\mu_g}{\hbar}\eta_g E^* - \frac{i\mu_g}{\hbar}\eta_g^* E + \frac{\Delta_{g0} - \Delta_g}{T_{1g}}, \quad (1c)$$

$$\frac{\partial \eta_a}{\partial t} = \frac{i\mu_a}{2\hbar}\Delta_a E - \frac{\eta_a}{T_{2a}}, \quad (1d)$$

$$\frac{\partial \Delta_a}{\partial t} = \frac{i\mu_a}{\hbar}\eta_a E^* - \frac{i\mu_a}{\hbar}\eta_a^* E + \frac{\Delta_{a0} - \Delta_a}{T_{1a}}, \quad (1e)$$

where the subscripts g and a in Eq. (1) represent gain and absorption, respectively. The independent variables z and t are length along the light-propagation axis of the QCL and time. The dependent variables E, $\eta_{g,a}$, and $\Delta_{g,a}$ refer to the envelopes of the electric field, gain polarization, and gain inversion. The parameters Δ_{g0} and Δ_{a0} refer to the equilibrium inversion away from the mode-locked pulse. The parameters n and c denote the index of refraction and the speed of light. The parameters $N_{g,a}\Gamma_{g,a}$ denote the effective electron density multiplied by the overlap factor. The parameters k, l, ϵ_0, and $\hbar$ denote the wave number in the active region, the linear loss including the mirror loss, the vacuum dielectric permittivity, and Planck's constant. The notation closely follows that of Wang et al. [17], with the differences that we have an absorbing as well as a gain medium, and we are considering unidirectional propagation, as is appropriate for a mode-locked pulse [28].

In order to achieve SIT mode locking, the growth of continuous waves must be suppressed. At the end of Sec. II, we briefly discussed possible approaches for seeding the mode locking. At this point, we make two observations. First, because continuous waves are suppressed, forward- and backward-propagating waves cannot interact, and spatial hole burning will not occur. Second, we did not include saturable absorption in Eq. (1) because we are not certain how to do so. This contribution was added phenomenologically to

the Maxwell-Bloch equations by Wang et al. [17] and Gordon et al. [18], based on experimental observations in particular QCLs and was attributed to effects that depend sensitively on the geometry of those QCLs. In future work, we will investigate the magnitude of the nonlinearity and chromatic dispersion that would impair SIT mode locking.

In order to suppress continuous waves, the gain must be below threshold. To derive this condition, we set $\Delta_g = \Delta_{g0}$ and $\Delta_a = \Delta_{a0}$ in steady state, where there is no evolution in z. We then find from Eqs. (1b) and (1d),

$$\eta_g = i\frac{\mu_g}{2\hbar}T_{2g}\Delta_{g0}E, \quad \eta_a = i\frac{\mu_a}{2\hbar}T_{2a}\Delta_{a0}E, \quad (2)$$

where we are considering continuous waves, so that there is no dependence on t and the t derivatives vanish. After substitution in Eq. (1a), we obtain in steady state

$$\frac{kN_g\Gamma_g\mu_g^2 T_{2g}\Delta_{g0}}{2\epsilon_0 n^2\hbar} + \frac{kN_a\Gamma_a\mu_a^2 T_{2a}\Delta_{a0}}{2\epsilon_0 n^2\hbar} - l = 0, \quad (3)$$

which may also be written $g\Delta_{g0} + a\Delta_{a0} - l = 0$, where

$$g = \frac{kN_g\Gamma_g\mu_g^2 T_{2g}}{2\epsilon_0 n^2\hbar}, \quad a = \frac{kN_a\Gamma_a\mu_a^2 T_{2a}}{2\epsilon_0 n^2\hbar}. \quad (4)$$

Physically, the parameter g corresponds to the gain per unit length from the gain periods of the QCL and the parameter a corresponds to the absorption per unit length from the absorbing periods. The condition for the linear gain to remain below threshold is $g\Delta_{g0} + a\Delta_{a0} - l < 0$. In the case of a fully inverted gain medium, so that $\Delta_g = \Delta_{g0} = 1$ and a fully uninverted absorbing medium so that $\Delta_a = \Delta_{a0} = -1$, the condition to suppress continuous waves becomes $g - a - l < 0$.

Assuming that T_{1g} and T_{1a} are large enough so that they may be set equal to ∞ in Eq. (1), and focusing on the special case in which $\mu_a = 2\mu_g$ and the pulse is a π pulse in the gain medium, Eq. (1) has an exact analytical solution that we may write as

$$E = \frac{\hbar}{\mu_g\tau}\text{sech } x, \quad (5a)$$

$$\eta_g = \frac{iB_g}{2}\Delta_{g0}\text{ sech } x, \quad (5b)$$

$$\Delta_g = B_g\Delta_{g0}\left(\frac{\tau}{T_{2g}} - \tanh x\right), \quad (5c)$$

$$\eta_a = \frac{iB_a}{2}\Delta_{a0}\left(-\text{ sech } x\tanh x + \frac{\tau}{3T_{2a}}\text{sech } x\right), \quad (5d)$$

$$\Delta_a = \frac{B_a}{2}\Delta_{a0}\left(1 + \frac{\tau^2}{3T_{2a}^2}\right) - B_a\Delta_{a0}\left(\text{sech}^2 x + \frac{2\tau}{3T_{2a}}\tanh x\right), \quad (5e)$$

where

$$x = \frac{t}{\tau} - \frac{z}{v\tau}, \qquad (6)$$

while

$$B_g = \frac{1}{1 + \tau/T_{2g}} \quad \text{and} \quad B_a = \frac{2}{(1 + \tau/3T_{2a})(1 + \tau/T_{2a})} \qquad (7)$$

are chosen such that $\Delta_g \rightarrow \Delta_{g0}$ and $\Delta_a \rightarrow \Delta_{a0}$ as $t \rightarrow -\infty$, so that the equilibrium population completely recovers on every pass of the pulse through the laser. Hence, Eq. (5) shows that stable mode-locked operation can be achieved in the proposed structure. The parameters τ and v that correspond to the pulse duration and the pulse velocity are determined by the equations

$$\frac{\tau/T_{2g}}{1 + \tau/T_{2g}} g\Delta_{g0} + \frac{\tau^2/3T_{2a}^2}{(1 + \tau/T_{2a})(1 + \tau/3T_{2a})} a\Delta_{a0} - l = 0 \quad (8)$$

and

$$\frac{1}{v} = \frac{n}{c} - a\tau \frac{\tau/2T_{2g}}{(1 + \tau/T_{2a})(1 + \tau/3T_{2a})} \Delta_{a0}. \qquad (9)$$

The full-width half-maximum pulse duration τ_{FWHM} equals 1.763τ. This solution was previously presented in the special case $\Delta_{g0} = 1$ and $\Delta_{a0} = -1$ [16]. We now consider in more detail the special case $T_{2g} = T_{2a} \equiv T_2$. Writing $\bar{g} = g/l$, $\bar{a} = a/l$, and $\bar{\tau} = \tau/T_2$, we find that the condition to suppress the growth of continuous waves becomes $\bar{g}\Delta_{g0} + \bar{a}\Delta_{a0} - 1 < 0$, and the equation for the pulse duration becomes

$$\frac{3}{\bar{\tau}} = \frac{3\bar{g}\Delta_{g0} - 4}{2} + \left[\left(\frac{3\bar{g}\Delta_{g0} - 4}{2} \right)^2 + 3(\bar{g}\Delta_{g0} + \bar{a}\Delta_{a0} - 1) \right]^{1/2}. \qquad (10)$$

Equation (10) only has a solution when $\bar{a} < (3\bar{g}\Delta_{g0} - 2)^2/12|\Delta_{a0}|$, where we note that $\Delta_{a0} < 0$.

The conditions for stability may be summarized as

$$\frac{(\bar{g}\Delta_{g0} - 1)}{|\Delta_{a0}|} < \bar{a} < \frac{(3\bar{g}\Delta_{g0} - 2)^2}{12|\Delta_{a0}|}. \qquad (11)$$

When $\bar{a}$ is above the upper limit in Eq. (11), we have found by solving Eq. (1) computationally that an initial pulse damps away. When $\bar{a}$ is below the lower limit, continuous waves grow. We have computationally found that multiple pulses are generated in this case.

Equation (11) defines a parameter regime in which stable mode-locked operation is possible. In Fig. 4, we present the stability limits when the population inversion in the gain and absorbing periods vary. In all cases, the lower lines indicate the limiting values for $\bar{a}$, below which continuous waves grow, and the upper lines indicate the limiting values for $\bar{a}$, above which initial pulses damp. Figure 4 shows that the minimum value of $\bar{g}$ that is required for stable operation increases when Δ_{g0} decreases and Δ_{a0} increases by the same amount. There is also a slight decrease in the lower limit for $\bar{a}$ and a larger decrease in the upper limit. Since the upper limit drops more than the lower limit, the stable parameter region becomes smaller. We also show contours of the pulse duration, normalized by the coherence time T_{2g}, denoted $\bar{\tau}$,
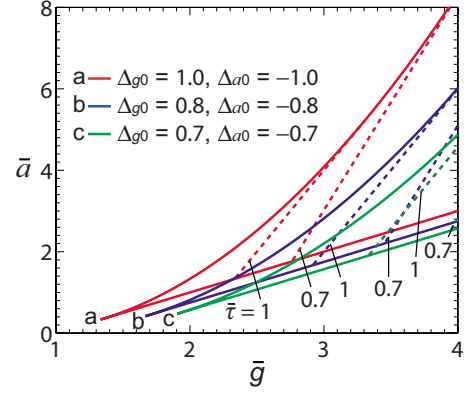

FIG. 4. (Color online) Stability limits of the normalized absorption ($\bar{a}$) vs the normalized gain ($\bar{g}$) coefficients with different Δ_{g0} and Δ_{a0}. The ratio T_1/T_2 is infinity in all cases. For a given $\bar{\tau}$ and $\bar{a}$, the required $\bar{g}$ increases as Δ_{g0} and $|\Delta_{a0}|$ decrease.

as given by Eq. (10). Pulse durations are approximately on the order of T_{2g} when $\bar{g} \approx 2.5$ and $\bar{a} \approx 2.0$. We also note that pulses become shorter as $\bar{g}$ and $\bar{a}$ increase. However, both $\bar{g}$ and $\bar{a}$ are directly proportional to the current; so, to increase the gain and absorption in a fixed ratio, one must increase the current. At the same time, we note that $\bar{g}$ and $\bar{a}$ are directly proportional to T_2. Hence, it is possible to reduce the required current by increasing T_2.

We have studied what happens to the stability limits if T_{2a}/T_{2g} vary and we show the results in Fig. 5. In Fig. 5, we have varied T_{2a} keeping T_{2g} constant. In a QCL, typical values of T_{2g} and T_{2a} are on the order of 100 fs. A change in T_{2a} affects the stability limits more than does a change in T_{2g} as is evident from Eq. (8). When T_{2a}/T_{2g} increases, the upper stability limits increase. When $\bar{g} = 4.0$, we find that the upper limit for $\bar{a}$ varies from 3.75 to 8.3 to 24 as T_{2a}/T_{2g} varies from 0.5 to 1.0 to 2.0. The lower limit for $\bar{a}$ remains unchanged.

We now derive an energy-balance equation that describes the energy input limits for stable operation when $\tau \ll T_2$. We define $\Theta(z,t) = \int_{-\infty}^{t} E(z,t')dt'$. Then, Eqs. (1b) and (1c) can be written as
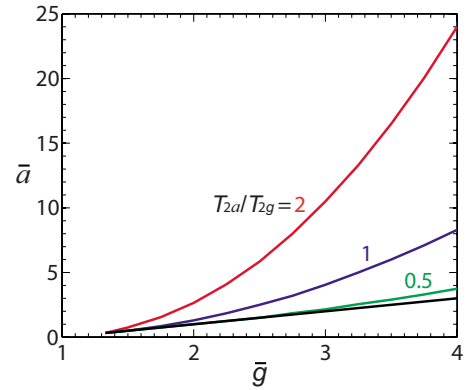

FIG. 5. (Color online) Stability limits of the normalized absorption ($\bar{a}$) vs the normalized gain ($\bar{g}$) coefficients with different T_{2a}/T_{2g}. We set $T_{1g} = T_{1a} = \infty$ in all cases. In equilibrium, the gain medium is completely inverted, i.e., $\Delta_{g0} = 1.0$, and the absorbing medium is completely uninverted, i.e., $\Delta_{a0} = -1.0$.

$$\frac{\partial \eta_g(z,t)}{\partial t} = \frac{i\mu_g}{2\hbar} \Delta_g(z,t) \frac{\partial \Theta(z,t)}{\partial t} \qquad (12)$$

and

$$\frac{\partial \Delta_g(z,t)}{\partial t} = 2 \frac{i\mu_g}{\hbar} \eta_g(z,t) \frac{\partial \Theta(z,t)}{\partial t}. \qquad (13)$$

In the gain medium, the polarization and population inversion can be written in terms of a single angle α as $2i\eta_g = \cos\alpha$ and $\Delta_g = \sin\alpha$. We integrate both sides of Eq. (12) or Eq. (13), after substituting these expressions for η_g and Δ_g and assuming that $\Delta_g(z,t \to -\infty) = 1$. We then obtain $\alpha(z,t) = \pi/2 + (\mu_g/\hbar)\Theta(z,t)$. We may similarly write $2i\eta_a = \cos\beta$ and $\Delta_a = \sin\beta$ in the absorbing medium, and we then find $\beta(z,t) = -\pi/2 + (\mu_a/\hbar)\Theta(z,t)$, where we have set $\Delta_a(z,t \to -\infty) = -1$. We now consider Eq. (1a) in steady state, where there is no evolution in z, and in the limit $t \to \infty$, where there is no evolution in t. We also define a normalized pulse energy

$$\bar{\theta}(z) = (\mu_g/\hbar)\Theta(z,t \to \infty). \qquad (14)$$

Equation (1a) now becomes

$$g \sin[\bar{\theta}(z)] = a \frac{\mu_g}{\mu_a} \frac{T_{2g}}{T_{2a}} \sin\left[\frac{\mu_a}{\mu_g} \bar{\theta}(z)\right], \qquad (15)$$

where we note that the linear loss may be neglected in the limit $\tau \ll T_2$. In the special case $\mu_a = 2\mu_g$ and $T_{2g} = T_{2a} \equiv T_2$, we find $a(\mu_g/\mu_a)(T_{2g}/T_{2a})\sin[(\mu_a/\mu_g)\bar{\theta}] = a\cos\bar{\theta}\sin\bar{\theta}$, so that Eq. (15) becomes $\cos\bar{\theta} = g/a$, which defines the limits of the input energy that is required to generate a single pulse,

$$\cos^{-1}(g/a) < \bar{\theta} < 2\pi - \cos^{-1}(g/a). \qquad (16)$$

When the initial value of $\bar{\theta}$ is within these limits, a single pulse with a final value of $\bar{\theta} = \pi$ is generated. When the initial value of $\bar{\theta}$ is below this value, the lower limit in Eq. (16), the initial pulse damps. When the initial value of $\bar{\theta}$ is above the upper limit, the initial pulse splits into multiple pulses.

In the analysis up to now it has been assumed that the central carrier frequency of the light pulse and the transition frequency in both the gain and absorbing media are the same. Since the frequency of the light is largely determined by the gain medium, it is reasonable to assume that there is no detuning between the light and the gain medium. Even if the mode locking is seeded by injection locking, analogous to the experiment of Choi et al. [20] the injection-locking laser can be tuned to the gain resonance. In principle, there may be a small detuning between the gain and absorbing media due to design or growth issues; however, it is possible to design the gain and absorbing media so that detuning is nearly absent. QCLs are currently being grown with high accuracy and experimentally observed wavelengths agree closely with the designed values.

If there is a detuning of Δ_ω between the gain and the absorbing periods and the light pulses are tuned to the gain periods, Eq. (1d) becomes

$$\frac{\partial \eta_a}{\partial t} = \frac{i\mu_a}{2\hbar} E\Delta_a - \left(\frac{1}{T_2} - i\Delta_\omega\right)\eta_a. \qquad (17)$$

Then the solutions for η_a and Δ_a change. Analytical solutions for η_a and Δ_a may be found in the presence of detuning Δ_ω when $\tau \ll T_2$, so that the term proportional to $1/T_2$ may be neglected in the polarization equation. Then, the solutions for η_a and Δ_a become

$$\eta_a = \frac{\Delta_\omega \tau}{1+(\Delta_\omega \tau)^2}\operatorname{sech} x + i\frac{1}{1+(\Delta_\omega \tau)^2}\operatorname{sech} x \tanh x, \qquad (18a)$$

$$\Delta_a = -1 + \frac{2}{1+(\Delta_\omega \tau)^2}\operatorname{sech} x, \qquad (18b)$$

where $x = t/\tau - z/v\tau$ and $\Delta_{a0} = -1$ at $t \to -\infty$.

On physical grounds, it is apparent that the criterion for acceptable detuning is that $\Delta_\omega \lesssim 1/T_2$, since $\tau \lesssim T_2$ and the bandwidth of the pulse in angular frequency is $\sim \tau^{-1}$. If T_2 is 100 fs, and we demand conservatively that $\Delta_\omega < 0.1/T_2$, then $\Delta_\omega \lesssim 10^{12}$ s^{-1}, corresponding to an allowed frequency detuning of 1.6×10^{11} Hz, which is 2% of the carrier frequency of 8 μm light and is not overly demanding.

V. SIMULATION RESULTS

In order for the solution reported in Eq. (5) to be of any practical interest, it must be robust when μ_a differs from $2\mu_g$, when T_{1g} and T_{1a} are on the order of a picosecond or less, when an initial pulse that is long compared to its final, stable duration is injected into the medium, and when the initial pulse area differs from the ideal value of π in the gain medium and 2π in the absorbing medium. The Maxwell-Bloch equations must be solved computationally to determine what happens under these conditions. For computational analysis, we normalize Eq. (1). We define $\bar{E} = (\mu_g T_{2g}/\hbar)E$ and we introduce the retarded time $t' = t - (n/c)z$, the normalized time $\bar{t} = t/T_{2g}$, and the normalized distance $\bar{z} = lz$, so that Eq. (1) becomes

$$\frac{\partial \bar{E}}{\partial \bar{z}} = -i\bar{g}\eta_g - i\frac{\bar{a}}{(T_{2a}/T_{2g})\bar{\mu}}\eta_a - \frac{1}{2}\bar{E}, \qquad (19a)$$

$$\frac{\partial \eta_g}{\partial \bar{t}} = \frac{i}{2}\Delta_g \bar{E} - \eta_g, \qquad (19b)$$

$$\frac{\partial \Delta_g}{\partial \bar{t}} = i(\eta_g \bar{E}^* - \eta_g^* \bar{E}) + \frac{\Delta_{g0} - \Delta_g}{T_{1g}/T_{2g}}, \qquad (19c)$$

$$\frac{\partial \eta_a}{\partial \bar{t}} = \frac{i}{2}\bar{\mu}\Delta_a \bar{E} - \frac{\eta_a}{T_{2a}/T_{2g}}, \qquad (19d)$$

$$\frac{\partial \Delta_a}{\partial \bar{t}} = i\bar{\mu}(\eta_a \bar{E}^* - \eta_a^* \bar{E}) + \frac{\Delta_{a0} - \Delta_a}{T_{1a}/T_{2g}}, \qquad (19e)$$

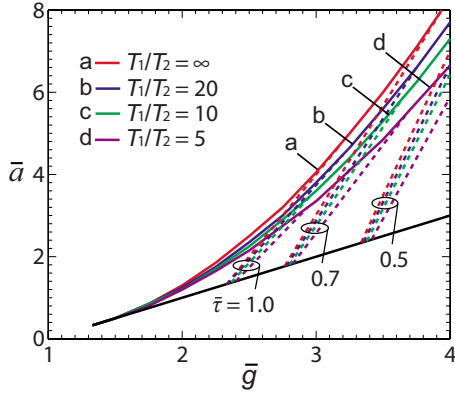where $\bar{g} = g/l$, $\bar{a} = a/l$, and $\bar{\mu} = \mu_a/\mu_g$.

FIG. 6. (Color online) Stability limits of the normalized absorption ($\bar{a}$) vs the normalized gain ($\bar{g}$) coefficients with different T_1/T_2. In equilibrium, the gain medium is completely inverted, i.e., $\Delta_{g0} = 1.0$ and the absorbing medium is completely uninverted, i.e., $\Delta_{a0} = -1.0$. In each bundle of dashed lines, corresponding to a fixed value of $\bar{\tau}$, T_1/T_2 decreases from left to right.

In our simulations, we used different window sizes, depending on the pulse evolution, and we verified that the pulse intensities are always zero at the window boundaries. We spaced our node points 1–5 fs apart, and we chose a step size between 1 and 10 μm, depending on the material parameters in the simulation. In each simulation these values were constant and we checked that reducing these values made no visible difference in our plotted results. Finally, we verified by extending the propagation length that we were following the pulses over a sufficiently long length to reliably determine whether the pulses are stable or not.

In Fig. 6, we show the limits of $\bar{g}$ and $\bar{a}$ for stable operation with different values of T_1/T_2 when $T_{1g} = T_{1a} \equiv T_1$ and $T_{2g} = T_{2a} \equiv T_2$. We begin by assuming that a hyperbolic-secant-shaped pulse having an area of π is injected into the QCL. Before the pulse is injected, the population is completely in the upper lasing state in the gain medium, i.e., $\Delta_{g0} = 1.0$ and is completely in the ground state in the absorbing medium, i.e., $\Delta_{a0} = -1.0$. In Fig. 6, the black solid line at the bottom defines the lower limits of $\bar{a}$ for any T_1/T_2. The solid curves on the top are the loss-limited boundaries for different values of T_1/T_2. The injected pulses are only stable when the gain and absorption parameters are set between these two boundary limits. Stable pulses propagate in the laser cavity with no change in shape and energy. We show the pulse evolution in the stable regime and unstable regimes

in Fig. 7. Figure 7(a) shows stable pulse evolution when $\bar{g}$ = 4.0 and $\bar{a}$ = 3.5. The laser becomes unstable when operated with $\bar{a}$ smaller than the lower limits given in Fig. 6 due to the growth of continuous waves. In this case, the net gain of the laser becomes positive, i.e., $\bar{g} - \bar{a} - 1 > 0$, and multiple pulses may form in the cavity, leading to the generation of multiple pulses in our simulations. We give an example of this behavior in Fig. 7(b). In this case, we set $\bar{g} = 4.0$ and $\bar{a} = 1.0$; the laser becomes unstable when $\bar{z} = 20$ and the laser cavity develops more than one pulse. With $\bar{a}$ greater than the upper limit, the gain medium cannot compensate for absorption and the linear loss. As a result, pulses damp. In Fig. 7(c), which exhibits this behavior, we have set $\bar{g} = 4.0$ and $\bar{a} = 7.8$. The upper limit for $\bar{a}$ decreases when T_1/T_2 decreases as shown in Fig. 6, because the damping increases. We also show contours of the stable normalized pulse duration, $\bar{\tau} = \tau_{\text{FWHM}}/(1.763 T_2)$, with dashed lines in Fig. 6. Pulse durations are on the order of T_2 when $\bar{g} \gtrsim 2.5$ and $\bar{a} \gtrsim 2.0$. The pulse durations can be made arbitrarily short by increasing $\bar{g}$ and $\bar{a}$. However, $\bar{g}$ and $\bar{a}$ are proportional to the current, so that the current must be increased. If T_1/T_2 decreases, then $\bar{g}$ must increase if $\bar{a}$ is constant in order to maintain $\bar{\tau}$ at a constant value.

As we discussed, in Sec. III, in a practical QCL design, we must have $T_{1g} > T_{1a}$. For generality, we consider here the stability limits as T_{1a}/T_{1g} varies between 0.5 and 2.0. Figure 8 shows the stability limits of $\bar{g}$ and $\bar{a}$ as T_{1a}/T_{1g} is varied. The solid black line at the bottom is the lower limit of $\bar{a}$ and remains the same for any T_{1a}/T_{1g}. However, the upper limit of $\bar{a}$ decreases when T_{1a}/T_{1g} decreases.

The analytical solution of the Maxwell-Bloch equations given in Eq. (5) assumes that the absorbing medium has a dipole moment twice that of the gain medium, i.e., $\mu_a = 2\mu_g$. The condition $\mu_a = 2\mu_g$ will not be exactly satisfied due to design constraints and growth limitations. The QCL gain is determined by μ_g and T_{1g}. To produce large gain, it is preferable that μ_g is large. In a vertical transition QCL, the dipole moment is generally $\gtrsim 2$ nm. In diagonal-transition QCLs, the dipole moment is $\gtrsim 1.4$ nm, which is smaller. Despite the smaller value of μ_g with diagonal transitions, we must have $\mu_a/e \gtrsim 2.8$ to satisfy the condition $\mu_a = 2\mu_g$. Therefore, it is useful in practice if SIT mode locking is possible when $\mu_a < 2\mu_g$. We determine the stability limits of $\bar{\mu} = \mu_a/\mu_g$ for stable operation. Figure 9 shows the lower and upper stability limits of $\bar{\mu}$ vs $\bar{g}$ as $\bar{a}$ varies. The solid lines in Fig. 9 indicate the lower limits for $\bar{\mu}$ while the dashed lines indicate the upper limits. The two ends of each of the lines
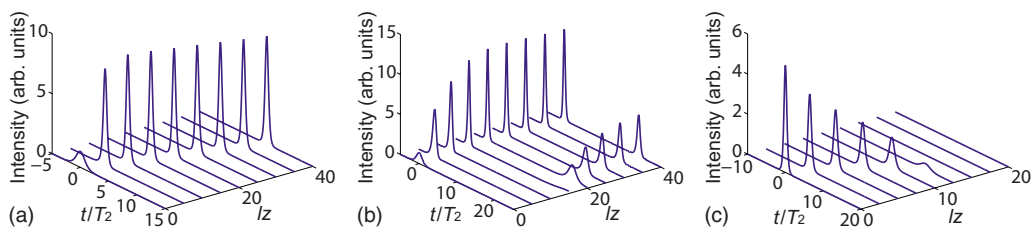

FIG. 7. (Color online) Pulse evolution in the system. (a) Gain and absorption coefficients are in the stable regime, $\bar{g} = 4.0, \bar{a} = 3.5$. (b) Gain and absorption coefficients are in the regime in which continuous waves are unstable, $\bar{g} = 4.0, \bar{a} = 1.0$. (c) Gain and absorption coefficients are in the regime where any initial pulse attenuates, $\bar{g} = 4.0, \bar{a} = 7.8$. The ratio T_1/T_2 equals 10 in all cases. In equilibrium, the gain medium is completely inverted, i.e., $\Delta_{g0} = 1.0$, and the absorbing medium is completely uninverted, i.e., $\Delta_{a0} = -1.0$.
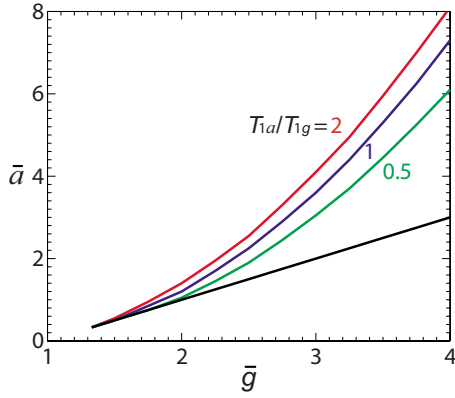
FIG. 8. (Color online) Stability limits of the normalized absorption ($\bar{a}$) vs the normalized gain ($\bar{g}$) coefficients with different values of T_{1a}/T_{1g}. We set $T_{2g}=T_{2a}$ and $T_{1g}/T_{2g}=10$ in all cases. In equilibrium, the gain medium is completely inverted, i.e., $\Delta_{g0}=1.0$, and the absorbing medium is completely uninverted, i.e., $\Delta_{a0}=-1.0$.

are at the stability boundaries for $\bar{g}$ at each particular $\bar{a}$. In each of the cases, the minimum value of $\bar{\mu}$ is approximately 2 when $\bar{g}$ is near its minimum, below which an input pulse attenuates. As $\bar{g}$ increases toward the limit at which continuous waves become unstable, the minimum value of $\bar{\mu}$ required for stable operation decreases significantly. Pulses are stable with $\bar{\mu} \sim 1.2$ when $\bar{g}=3.5$, 4.0, and 4.5 with $\bar{a}=2.5$, 3.0, and 3.5, respectively, with $\bar{g}$ just below the stability limit for generating continuous waves. However, the stable pulse duration increases significantly as $\bar{\mu}$ decreases. When $\bar{\mu}$ is below the solid lines in Fig. 9, pulses attenuate. The minimum value of $\bar{\mu}$ required for stable operation increases as $\bar{a}$ increases for any fixed $\bar{g}$. We have found no hard upper limit to stability as $\bar{\mu}$ increases, although the pulses are increasingly distorted. The dashed lines in Fig. 9 indicate the values of $\bar{\mu}$ at which the pulses become double peaked.

We have derived an energy balance equation in Eq. (16) that defines the limits of the input energy for stable operation. However, Eq. (16) assumes that input pulse has a dura-
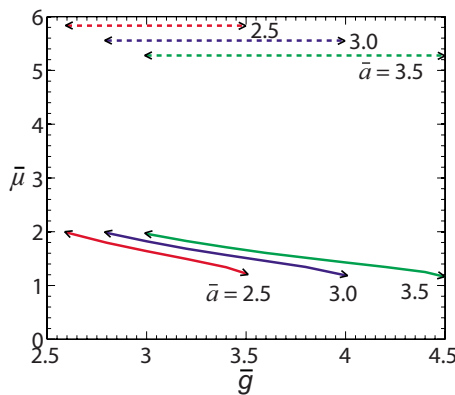

FIG. 9. (Color online) Stability limits of the ratio of the dipole moments in the absorbing and gain media ($\bar{\mu}$) vs the normalized gain coefficient ($\bar{g}$) for three cases of normalized absorption ($\bar{a}$). The ratio T_1/T_2 is 10 in all cases. In equilibrium, the gain medium is completely inverted, i.e., $\Delta_{g0}=1.0$, and the absorbing medium is completely uninverted, i.e., $\Delta_{a0}=-1.0$.
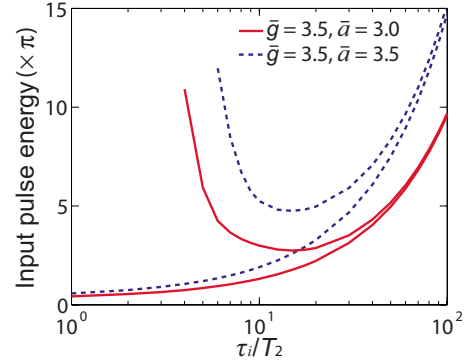

FIG. 10. (Color online) Input pulse energy limits vs normalized input pulse duration (τ_i/T_2) for two different cases of $\bar{g}$ and $\bar{a}$. In both the cases, we set $T_1/T_2=10$. In equilibrium, the gain medium is completely inverted, i.e., $\Delta_{g0}=1.0$, and the absorbing medium is completely uninverted, i.e., $\Delta_{a0}=-1.0$.

tion, $\tau_i=\tau_{FWHM}/1.763 \ll T_2 \ll T_1$, so that the effects of a finite coherence time T_2 and damping due to finite T_1 may be ignored. If this condition is not satisfied, then Eq. (16) is no longer valid. From a practical standpoint, an input pulse having a duration on the order of T_2 or longer than T_2 is advantageous. We have calculated the dependence of the minimum and maximum input energy on the input pulse duration for two different combinations of gain and loss. We show the results in Fig. 10. The input pulse duration is normalized to $T_2=T_{2g}=T_{2a}$ and is plotted on a logarithmic scale. The value of T_1/T_2 has been set to 10. When $\tau_i/T_2=0.1$, we find that the minimum normalized energy $\bar{\theta}=(\mu_g/\hbar)\int_{-\infty}^{\infty} E dt=\int_{-\infty}^{\infty} \bar{E} d\bar{t}$ that is required for stable operation is 0.30π when $\bar{g}=3.5$ and $\bar{a}=3.0$. However, as we increase τ_i/T_2, the minimum normalized pulse energy that is required for stable operation increases significantly due to the pulse's decorrelation over its duration. It increases to 0.42π when $\tau_i/T_2=1$, 1.31π when $\tau_i/T_2=10$, and 9.59π when $\tau_i/T_2=100$. Pulses are stable for an input energy of at least 20π when $\tau_i/T_2 \lesssim 3$.

We find that pulses split into multiple pulses when the input pulse energy is $\gtrsim 2\pi$. However, at the stable pulse duration $\bar{\tau} \sim 0.5$ for the parameters $\bar{g}=3.5$, $\bar{a}=3.0$, only one pulse is stable, and the others damp even with an initial normalized energy of 20π when $\tau_i/T_2 < 4$. When $\tau_i/T_2 \gtrsim 4$, continuous waves become unstable. We find that multiple pulses are generated when the input energy is $\geq 3\pi$ with $\tau_i/T_2=10$. The upper stability limit for the input energy decreases as τ_i/T_2 increases when $\tau_i/T_2 \lesssim 10$. However, beyond that point, the upper stability limit increases with τ_i/T_2 as damping due to T_1 comes into effect. The stability limits for the input normalized energy when $\bar{g}=3.5$ and $\bar{a}=3.5$ show a similar trend with the exception that both the stability limits are shifted upward due to an increase in absorption.

We simulated a number of cases in which we investigated the effect of detuning the absorbing medium from the gain medium and the carrier frequency of the light. Setting $T_1/T_2=10$, $\Delta_{g0}=1.0$, and $\Delta_{a0}=-1.0$, we found that stable operation can be obtained with a detuning $\Delta_\omega T_2 \leq 0.53$ when $\bar{g}=3.5$, $\bar{a}=3.5$. Stable operation can be obtained with $\Delta_\omega T_2 \leq 0.36$ when $\bar{g}=3.5$, $\bar{a}=3.0$, and with $\Delta_\omega T_2 \leq 0.15$ when $\bar{g}=3.5$, $\bar{a}=2.5$.

VI. DISCUSSION

In prior work [16], we showed that by combining absorbing with gain periods in a QCL, one can create nearly ideal conditions to observe SIT mode locking and thereby obtain pulses that are less than 100 fs long from a midinfrared laser. In this work, we extend our prior analytical work, and we present detailed computational studies of the Maxwell-Bloch equations, in which we extensively investigated the stability of the solutions as the equation parameters vary. The solutions demonstrate the robustness of the SIT mode-locking technique and that QCLs can be mode-locked using the SIT effect within practically achievable parameter regimes.

The unidirectional, two-level Maxwell-Bloch equations that we have used in our study are a good starting point for the investigation of SIT mode locking. However, effects that are not included in the model are expected to affect the stability limits. First, it is not possible to determine the effect of edge reflections with a unidirectional model and we cannot realistically investigate the consequences when continuous waves become unstable. For that reason, we have implemented a bidirectional model like that of Wang *et al.* [17] and Gordon *et al.* [18], but keeping both gain and absorbing media. We found, as expected, that spatial hole burning is not present when continuous waves are below threshold, but can become important when continuous waves become unstable. We also found that edge effects change the stability limits somewhat. These results will be presented elsewhere. Sec-ond, nonlinear saturation and chromatic dispersion will set limits on the validity of our theory as they become large. The results of Wang *et al.* [17] and Gordon *et al.* [18] indicate that these effects are not large enough in practice to seriously impact the validity of our model, but the limits that these effects impose merits further study. Third, real QCLs have multiple levels in the active region and the effect of several relaxation times on the stability limits remains to be explored. Finally, we have seen in Fig. 5 that the stability limits depend sensitively on the ratios of the coherence times in the gain and absorbing media. Calculating the actual values of T_{2g} and T_{2a} is thus important.

In this work, we have treated g and a as parameters. While we expect them both to increase proportional to the current, it is important to calculate the contributions of the individual gain and absorbing periods, shown in Fig. 3, to g and a respectively, so that we know how many of each kind of period should be grown. These calculations require a complete calculation of the carrier distribution and coherence times in all the QCL levels.

[1] S. L. McCall and E. L. Hahn, Phys. Rev. Lett. **18**, 908 (1967).

[2] S. L. McCall and E. L. Hahn, Phys. Rev. **183**, 457 (1969).

[3] H. M. Gibbs and R. E. Slusher, Appl. Phys. Lett. **18**, 505 (1971).

[4] R. Bonifacio and L. M. Narducci, Lett. Nuovo Cimento **1**, 671 (1969).

[5] M. H. Crowell, IEEE J. Quantum Electron. **1**, 12 (1965).

[6] T. Uchida and A. Ueki, IEEE J. Quantum Electron. **3**, 17 (1967).

[7] A. G. Fox and P. W. Smith, Phys. Rev. Lett. **18**, 826 (1967).

[8] P. W. Smith, IEEE J. Quantum Electron. **3**, 627 (1967).

[9] A. Frova, M. A. Duguay, C. G. B. Garrett, and S. L. McCall, J. Appl. Phys. **40**, 3969 (1969).

[10] V. V. Kozlov, Pis'ma Zh. Eksp. Teor. Fiz. **69**, 906 (1999) [JETP Lett. **69**, 906 (1999)].

[11] H. A. Haus, J. Appl. Phys. **46**, 3049 (1975).

[12] V. V. Kozlov, Phys. Rev. A **56**, 1607 (1997).

[13] H. Risken and K. Nummedal, J. Appl. Phys. **39**, 4662 (1968); R. Graham and H. Haken, Z. Phys. **213**, 420 (1968).

[14] J. Faist, F. Capasso, D. Sivco, C. Sirtori, A. Hutchinson, and A. Cho, Science **264**, 553 (1994).

[15] C. Sirtori and R. Teissier, in *Quantum Cascade Lasers: Overview of Basic Principles of Operation and State of the Art*, Intersubband Transitions in Quantum Structures, edited by R. Paiella (McGraw-Hill, New York, 2006).

[16] C. R. Menyuk and M. A. Talukder, Phys. Rev. Lett. **102**, 023903 (2009).

[17] C. Y. Wang, L. Diehl, A. Gordon, C. Jirauschek, F. X. Kärtner, A. Belyanin, D. Bour, S. Corzine, G. Höfler, M. Troccoli, J. Faist, and F. Capasso, Phys. Rev. A **75**, 031802(R) (2007).

[18] A. Gordon, C. Y. Wang, L. Diehl, F. X. Kärtner, A. Belyanin, D. Bour, S. Corzine, G. Höfler, H. C. Liu, H. Schneider, T. Maier, M. Troccoli, J. Faist, and F. Capasso, Phys. Rev. A **77**, 053804 (2008).

[19] C. Y. Wang, L. Kuznetsova, L. Diehl, F. Kärtner, M. A. Belkin, H. Schneider, H. C. Liu, and F. Capasso, Proceedings of the 2008 Conference on Lasers and Electro-Optics, http://www.opticsinfobase.org/abstract.cfmURI=CLEO-2008-CPDA11.

[20] H. Choi, V.-M. Gkortsas, F. X. Kärtner, L. Diehl, C. Y. Wang, F. Capasso, D. Bour, S. Corzine, J. Zhu, G. Höfler, and T. B. Norris, Proceedings of the 2008 Conference on Lasers and Electro-Optics, http://www.opticsinfobase.org/abstract.cfmURI=CLEO-2008-CTuP7

[21] M. F. Pereira, Jr., S.-C. Lee, and A. Wacker, Phys. Rev. B **69**, 205310 (2004).

[22] T. Kubis, C. Yeh, and P. Vogl, Phys. Status Solidi C **5**, 232 (2008).

[23] I. Savić, N. Vukmirović, Z. Ikonić, D. Indjin, R. W. Kelsall, P. Harrison, and V. Milanović, Phys. Rev. B **76**, 165310 (2007).

[24] R. Nelander, A. Wacker, M. F. Pereira, Jr., D. G. Revin, M. R. Soulby, L. R. Wilson, J. W. Cockburn, A. B. Krysa, J. S. Roberts, and R. J. Airey, J. Appl. Phys. **102**, 113104 (2007).

[25] M. A. Talukder and C. R. Menyuk, Proceedings of the International Quantum Cascade Lasers School and Workshop, Monte Verita, Switerland, 2008.

[26] L. Allen and J. H. Eberley, *Optical Resonance and Two Level Atoms* (Dover, New York, 1987).

[27] R. W. Boyd, *Nonlinear Optics*, 2nd ed. (Academic Press, London, 2003).

[28] H. A. Haus, IEEE J. Sel. Top. Quantum Electron. **6**, 1173 (2000).